Time-dependent development of flow instabilities of non-Newtonian melts and suspensions with rigid particles

Proceedings of AICHE Annual Meeting Austin, Texas

November 8, 2004

H. S. Tang* and D. M. Kalyon **

Stevens Institute of Technology

Hoboken, NJ 07030, USA

* Presently with Battelle Seattle Research Center, 1100 Dexter Av., Seattle, WA 98109

** dkalyon@stevens.edu

Key words : flow instabilities, wall slip, extrudate, and surface irregularities

1. Introduction

Flow instabilities are widely encountered during the extrusion of non-Newtonian fluids through various types of dies. Flow instabilities are manifested during extrusion by the occurrence of various types of distortions of the surface or the bulk of the extrudates, sometimes accompanied with time-dependent fluctuations in the pressure necessary to drive the flow under constant volumetric flow rate conditions. Various types of distortions of the extrudates are referred to as melt facture, shark skin, gross surface irregularities, spurt flow, slip/stick flow. The occurrences of such distortions of extrudates present bottlenecks, i.e., upper limits to the manufacturing rates in extrusion based processing of polymers and polymeric suspensions. Consistent with its industrial importance it has received significant academic and industrial attention [Benbow and Lamb (1963); Petrie and Denn (1976); Denn (2001); Kalyon and Gevgilili (2003)]. However, as suggested by Denn (2001), the instability phenomenon remains as an issue that is far from being clearly understood.

Capillary and slit die flows are often used as prototypes for studying the development of flow instabilities [see, for example, Lim and Schowalter (1989), Donlder et al. (1998), and Ovaici etc (1998)]. Previous studies have indicated that compressibility of the melt and slip at the wall are two important factors leading to the instabilities. Particularly, it was suggested that the discontinuity in the wall slip velocity versus wall shear stress relationships can lead to the onset of flow instabilities [Hatzikiriakos and Dealy (1992a), or (1992b)?]. Other studies have suggested that the flow instabilities can occur on the

negative-slope branch, e.g., during which the slip velocity decreases as wall stress increases [Georgiou (2003)].

This study is a continuation of our earlier studies [Kalyon and Gevgilili (2003) and Kalyon et al. (2003)] which aim at probing the effects of the flow boundary condition at the wall on the development of flow instabilities and extrudate surface irregularities upon the extrusion of polymer melts and polymeric suspensions. In these earlier studies the wall slip and flow instability behavior of two polymers, i.e., a poly (dimethyl siloxane), PDMS and an oxetane based alternating block thermo plastic elastomer BAMO/AMMO-TPE were studied along with the wall slip and flow instability behavior of PDMS filled with 10, 20, 40% by volume of hollow glass spheres and 60% by volume of KCl Filled BAMO/AMMO- TPE. Steady torsional flow was used in conjunction with the straight-line marker technique to analyze wall slip in steady torsional flow. Thermal imaging and high-speed cinematography were used with capillary flow to characterize the surface features of extrudates emerging from capillary dies. The effects of the convergence angle from the reservoir into the capillary die were also investigated (15, 45 and 75°) for unfilled PDMS and 10% glass filled PDMS. It was determined that the angle of convergence of the capillary die had no effect on the development of surface irregularities for these materials.

The incorporation of the glass filler into the PDMS binder gave rise to a reduction of the apparent shear rate range over which gross surface irregularities were observed. Furthermore, the extrudates of PDMS with the greatest solid loading level of our

study, i.e., 40% by volume spherical glass were largely free from surface irregularities except at relatively very low apparent shear rates. On the other hand, BAMO/AMMO elastomer melt, which exhibits stable stick over relatively high strains and shear rates in steady torsional flow does not exhibit surface irregularities in the same shear rate range in capillary flow [Kalyon and Gevgilili (2003)]. However, the incorporation of rigid particles into the BAMO/AMMO elastomer gives rise to flow instabilities and surface irregularities during extrusion.

 These earlier results suggested that the mechanisms for the development of surface irregularities of the extrudates of polymers and polymeric suspensions appear to depend on the stability of the wall boundary condition. Our hypothesis was that if a stable stick condition or a stable wall slip condition prevails at the wall over a broad range of shear rates, then flow instabilities are not observed over the same shear rate range. However, if there is a transition from a stick to slip or slip to stick condition then flow instabilities are experimentally observed at the transition point.

Our previous work has also shown that the wall slip behavior of polymers and polymeric suspensions is significantly affected by the amount of air entrained into the melt [Aral and Kalyon (1995); Kalyon et al. (1995)]. This intuitively suggests that the wall slip behavior would be a function of pressure due to the compressibility of the melt and the air it contains, as indeed found to be the case by Dealy and co-workers [Hatzikiriakos and Dealy (1992b)]. Following up on the compressibility and wall slip issues recently, we have derived analytical solutions for steady compressible capillary

and slit flows of generalized Newtonian fluids subject to pressure-dependent wall slip. These solutions show that, with the slip coefficient assumed to be inversely proportional to pressure, slip velocity increases in the flow direction and the flow can become a plug flow at the exit of the die.

This present paper extends the steady analysis to the time-dependent analysis of the extrusion flow subject to pressure dependent wall slip condition. As experimental evidence we will use results from our previous studies focusing on an unfilled poly(dimethyl siloxane), PDMS, melt and PDMS filled with 40% by volume of glass spheres [Kalyon and Gevgilili (2003); Kalyon et al. (2003)].

II. Experiments

Materials

The poly(dimethyl siloxane), PDMS, was procured from GE (GE Silicones-SE-30). It has a density of 980 kg/m^3 at ambient temperature and a zero shear viscosity of 28,900 Pa-s at 30 ºC. The filler particles consisted of spherical hollow glass particles with a specific gravity of 1.09 and an arithmetic mean particle diameter of 12 μm (Potters Industry).

Experimental apparati and procedures

An Advanced Rheometric Expansion System (ARES) rheometer, from Rheometric Scientific, Inc., Piscataway, NJ (currently TA Instruments), was utilized in

conjunction with steady torsional flow using cone-and-plate and parallel-disk configurations. The environmental chamber was equipped with an imaging window and auxiliary optics for continuous monitoring of the free surface of the specimen [Aral and Kalyon (1994); Gevgilili and Kalyon (2001)]. A high-speed camera, capable of recording at filming speeds as high as 2,000 frames per second, was part of the set-up.

During steady torsional flow a straight-line marker was placed on the edges of the cone/plate and the free surface of the polymer melt to enable the characterization of the wall slip velocity and the true deformation rate [Kalyon et al. (1993), Aral and Kalyon (1994); Gevgilili and Kalyon (2001)]. The discontinuities that develop between the surface of the plates of the rheometer and the bulk of the melt suggest the initiation of wall slip. The steady wall slip velocity values determined using the straight-line marker technique agree well with the steady wall slip velocity values determined upon the analysis of the dependence of the shear stress on the surface to volume ratio of the rheometer, i.e., the conventional Mooney technique [Kalyon et al. (1993)]. The steady torsional flow behavior of the PDMS and filled PDMS was characterized at various shear rates and temperatures to determine the conditions under which the catastrophic failure of the no-slip condition became apparent.

An Instron capillary rheometer was employed to collect additional shear viscosity data and to study the development of extrudate distortions upon exit from the die. The diameters, length over the diameter ratios and the converging angle of the tapered entry geometry connecting the reservoir of the barrel of the rheometer to the straight land

section of the capillary die were changed systematically. The shapes of the extruded samples, immediately upon extrusion from the die, were captured using a high-speed camera to allow the immediate characterization of the surfaces of the extrudates. The surface temperature distributions of the extrudates emerging from the die were also monitored using a ThermaCam thermal imaging camera. The temperature of the material immediately upon exit provided data on the effect of viscous energy dissipation and allowed the determination of the true temperature of the melt.

Experimental results

In case of unfilled PDMS steady torsional flow, used with the straight-line marker technique, suggests that PDMS exhibits strong wall slip (which is observed as a discontinuity in the marker line at the melt/wall interfaces) in the neighborhood of 0.07 MPa (Figure 1). Previous studies with the same PDMS have indicated that this critical shear stress, at which strong wall slip is initiated, is temperature independent [Kalyon and Gevgilili (2003)].

The various types of extrudate distortions observed with the unfilled PDMS as a function of the flow conditions are shown in Figure 2. The wall shear stress values were Bagley corrected by using a series of capillaries with systematically-varied length over diameter ratios of 1, 20 and 40 (or 60). At shear stress values greater than 0.07 MPa severe extrudate surface and bulk distortions were observed for PDMS. This wall shear stress coincides with the critical wall shear stress in steady torsional flow at which wall slip is onset. In the relatively low shear rate range the extrudates

of PDMS become undistorted and smooth, and the pressure monotonically increases to its steady state value. Over a transition region of 0.04 to 0.07 MPa the surfaces of the extrudates become relatively rough but the bulk is not distorted.

Similar experiments were carried out on PDMS suspensions filled with 10-40% by volume of glass spheres. The typical results for PDMS suspension with 40% by volume glass are shown in Figures 3 and 4. Figure 3 shows the typical steady torsional flow results for the 40% glass filled PDMS. Strong wall slip, as evidenced by the discontinuities in the straight-line marker occurring at the suspension/wall interface, occur at a critical wall shear stress range of about 0.029 MPa to 0.035 MPa for the 10-40% by volume glass filled PDMS suspensions. This critical wall shear stress is thus smaller than the critical wall shear stress value associated with the onset of strong wall slip observed for the unfilled PDMS.

The capillary flow curves for the 40% glass filled PDMS and the extrudates emerging from the capillary under various conditions are shown in Figure 4. The extrudates shown in the inserts were collected using four capillary dies with a constant length over diameter ratio of 40 and with diameters of 0.0328" (.83 mm), 0.059" (1.5 mm), 0.0984" (2.5 mm) and 0.1378" (3.5 mm) and a length over diameter ratio of 60 at a diameter of 2.5 mm. The wall shear stress values were Bagley corrected by using a series of capillaries with systematically varied length over diameter ratios of 1, 20 and 40 (or 60). The surface to volume dependence of the flow curves of 40% glass filled PDMS are clearly seen, i.e., with increasing surface to volume ratio (decreasing

diameter of the capillary die) the wall shear stress decreases at constant apparent shear rate suggesting wall slip. Over a broad range of shear rates the extrudates of the 40% glass filled PDMS are smooth and completely free of any type of surface irregularities. However, at relatively very small shear rates in the range of 0.5 1/s and less, and for the capillary with the length over the diameter ratio of 60, the surfaces of the extrudates become distorted. It is interesting to note that the wall shear stress values at which this surface irregularities are observed are smaller than the critical wall shear stress value of the suspension at which strong wall slip is onset in steady torsional flow (0.035 MPa).

The comparisons of Figs. 2 and 4 suggest that the surfaces of unfilled PDMS are free of distortions in the low shear rate range but become distorted at shear stresses which are generally above 0.07 MPa with some relatively minor surface roughnesses setting in over a transition region (0.04 MPa to 0.07 MPa). On the other hand, for the 40% filled PDMS the extrudates are free of surface and bulk irregularities over a broad range of shear rates and shear stresses but distortions set in at wall shear stress values, which are smaller than about 0.035 MPa. Thus, the flow instability behavior is reversed between the unfilled and filled PDMS.

The purpose of the paper is to present a mathematical model of the flow in a capillary die (Figure 5) and apply it to the extrusion of unfilled PDMS and 40% PDMS. The two fluids are considered to be compressible. The flow is isothermal, time-dependent and subject to wall slip with strong slip onset at the critical shear stress. The objective was to

determine if the consideration of the compressibility and the wall slip behavior of the PDMS melt and its suspension are sufficient to predict the conditions under which flow instabilities for PDMS and its suspensions are onset. Consistent with the earlier literature on the subject [Hatzikiriakos and Dealy (1992a); Georgiou, (2003)] the viscoelasticity of the melt and the suspension is ignored (this would have introduced various types of numerical instabilities which would not have allowed us to probe the effects of compressibility and wall slip alone) and the fluids are considered to behave as generalized Newtonian fluids flowing under lubrication flow conditions.

III. Simulation of the Time-dependent Flow Field

Mathematical models

The materials of the study, i.e., PDMS and the filled PDMS are considered to be compressible:

$$\boldsymbol{r} = \boldsymbol{g}\, p + \boldsymbol{g}_1 , \qquad\qquad (1)$$

where $\boldsymbol{r}$ is the density, p is the pressure, $\boldsymbol{g}$ and $\boldsymbol{g}_1$ are constants. The flow is considered to be subject to wall slip using a non-linear relationship between the slip velocity and shear stress [Yilmazer and Kalyon (1989); Zhang et al. (1995)]:

$$u_z = \boldsymbol{b}\, \boldsymbol{t}_{rz}^{\,sb} , \qquad\qquad (2)$$

which is further modified to include the concept of a critical wall shear stress above which strong wall slip is observed:

$$u_S = \beta \tau_W{}^{sb}(1 + \tanh(\alpha(\tau_W - \tau_a))). \tag{3}$$

Here, u_s is the slip velocity, t_w is the wall shear stress, t_a is the critical wall shear stress at which strong slip occurs, b is the Navier's slip coefficient, sb is an empirical constant, and a is a positive constant. When $t_w < t_a$, the slip velocity is assumed to be negligible, while for $t_w > t_a$, wall slip becomes significant.

The assumptions of the analysis were: 1) the flow is axis-symmetrical, 2) pressure changes only in the axial, z-direction, 3) the convection term and temperature effects from the continuity and momentum equations are ignored, 4) only the straight land section of the tube die is considered and thus the converging section of the capillary die is ignored. With these assumptions the equations of continuity and momentum become:

$$\frac{\partial p}{\partial t} + \frac{\partial}{\partial z}\left[\left(p + \frac{g_1}{g}\right)V\right] = 0,$$

$$\tag{4}$$

$$\frac{\partial V}{\partial t} + \frac{2t_w}{(gp + g_1)R} + \frac{1}{gp + g_1}\frac{\partial p}{\partial z} = 0,$$

where V is the cross section averaged velocity and t is time.

In this study, viscoelastic effects are ignored and PDMS and filled PDMS are taken to be generalized Newtonian fluids, with their shear viscosity behavior represented by the Herschel-Bulkley fluid. It is assumed that the wall stress can be calculated from steady flow as follows:

$$t_w = -\frac{R}{2}\left(\frac{\partial p}{\partial z}\right)_s \tag{5}$$

It should be noted that Hatzikiriakos and Dealy (1992b) have shown that a second term involving the derivative of the wall shear stress with axial distance in the circular tube needs to be added to take into consideration of the normal stress differences under lubrication flow conditions. However, this term was found to be negligible for our polymer and its suspensions.

The generalized Newtonian fluid with Herschel-Bulkley model is:

$$\begin{cases} t_{yz} = -m\left|\dfrac{\partial u_z}{\partial y}\right|^{n-1}\dfrac{\partial u_z}{\partial y} \pm t_y, & |t_{yz}| > t_y, \\ \dfrac{\partial u_z}{\partial y} = 0, & |t_{yz}| \leqslant t_y. \end{cases} \tag{6}$$

where t_y is the yield stress, m is the consistency index and n is the power law index. Equation (5) reduces to a power law fluid model when $t_y = 0$.

Under steady state flow conditions the solution for the mean velocity, V,

$$
V = \begin{cases}
\begin{aligned}
&-\frac{16\tau_y}{R^2 m^{1/n}(1+1/n)(3+1/n)}\left[-\tau_y - \frac{R}{2}\left(\frac{\partial p}{\partial z}\right)_s\right]^{2+1/n}\left(-\frac{\partial p}{\partial z}\right)_s^{-3}\\
&-\frac{16}{R^2 m^{1/n}(1+1/n)(2+1/n)}\left[-\tau_y - \frac{R}{2}\left(\frac{\partial p}{\partial z}\right)_s\right]^{3+1/n}\left(-\frac{\partial p}{\partial z}\right)_s^{-3}\\
&+\frac{16\tau_y}{m^{1/n}(1+1/n)}\left[-\tau_y - \frac{R}{2}\left(\frac{\partial p}{\partial z}\right)_s\right]^{1+1/n}\left(-\frac{\partial p}{\partial z}\right)_s^{-1}\\
&+\beta\left[-\frac{R}{2}\left(\frac{\partial p}{\partial z}\right)_s\right]^{sb}\left[1+1\tanh\left(\alpha\left(-\frac{R}{2}\left(\frac{\partial p}{\partial z}\right)_s - \tau_a\right)\right)\right], & \frac{R}{2}\left(\frac{\partial p}{\partial z}\right)_s > \tau_y,\\[2em]
&\beta\left[-\frac{R}{2}\left(\frac{dp}{dz}\right)_s\right]^{sb}\left[1+1\tanh\left(\alpha\left(-\frac{R}{2}\left(\frac{\partial p}{\partial z}\right)_s - \tau_a\right)\right)\right], & \frac{R}{2}\left(\frac{\partial p}{\partial z}\right)_s \leq \tau_y.
\end{aligned}
\end{cases}
$$

(7)

The boundary conditions for the flow are given as the following at the entry and exit planes of the tube:

$$V = V_0, \qquad z = 0.$$

(8)

$$p = p_a, \qquad z = L,$$

and the initial condition is set as a pseudo-steady flow. In summary, the flow problem in this study is formulated as Equations. 3-8.

Numerical methods

The flow domain was covered by a uniform grid with nodes $i=1,2,3,...,I$. The staggered mesh method is employed and the predictor-corrector scheme is used to discretize the above governing equations, that is:

Prediction:

$$\frac{\hat{p}_{i+1/2} - p_{i+1/2}^l}{\Delta t} + \frac{\left((p_{i+3/2}^l + p_{i+1/2}^l)/2 + g_1/g\right)V_{i+1}^l - \left((p_{i+1/2}^l + p_{i-1/2}^l)/2 + g_1/g\right)V_i^l}{\Delta z} = 0$$

$$\frac{\hat{V}_i - V_i^l}{\Delta t} + \frac{2t_{wi}^l}{\left(g(p_{i-1/2}^l + p_{i+1/2}^l)/2 + g_1\right)R} + \frac{1}{\left(g(p_{i-1/2}^l + p_{i+1/2}^l)/2 + g_1\right)}\frac{p_{i+1/2}^l - p_{i-1/2}^l}{\Delta z} = 0$$

$$(9)$$

$$t_{wi}^l = -\frac{R}{2}\left(\frac{\partial p}{\partial z}\right)_{si}^l$$

$$V_i^l = F\left[\left(\frac{\partial p}{\partial z}\right)_{si}^l\right]$$

where Δt is the time step, Δz is the grid spacing, l is the time step index, and F is the function defined as the RHS of Eq. (7).

Correction:

$$\frac{p_{i+1/2}^{l+1} - p_{i+1/2}^{l}}{\Delta t} + \frac{\left((p_{i+3/2}^{l} + p_{i+1/2}^{l})/2 + g_1/g\right)V_{i+1}^{l} - \left((p_{i+1/2}^{l} + p_{i-1/2}^{l})/2 + g_1/g\right)V_{i}^{l}}{2\Delta z}$$

$$+ \frac{\left((\hat{p}_{i+3/2} + \hat{p}_{i+1/2})/2 + g_1/g\right)\hat{V}_{i+1} - \left((\hat{p}_{i+1/2} + \hat{p}_{i-1/2})/2 + g_1/g\right)\hat{V}_{i}}{2\Delta z} = 0$$

$$\frac{V_{i}^{l+1} - V_{i}^{l}}{\Delta t} + \frac{2t_{wi}^{l}}{\left((\hat{p}_{i+3/2} + \hat{p}_{i+1/2})/2 + g_1/g\right)R} + \frac{2t_{wi}}{\left((\hat{p}_{i+3/2} + \hat{p}_{i+1/2})/2 + g_1/g\right)R}$$

$$+ \frac{1}{\left(g(p_{i-1/2}^{l} + p_{i+1/2}^{l})/2 + g_1\right)} \frac{p_{i+1/2}^{l} - p_{i-1/2}^{l}}{\Delta z} + \frac{1}{\left(g(\hat{p}_{i-1/2} + \hat{p}_{i+1/2})/2 + g_1\right)} \frac{\hat{p}_{i+1/2} - \hat{p}_{i-1/2}}{\Delta z} = 0$$

$$(10)$$

$$t_{wi} = -\frac{R}{2}\left(\frac{\partial \hat{p}}{\partial z}\right)_{si}$$

$$\hat{V}_{i} = F\left[\left(\frac{\partial \hat{p}}{\partial z}\right)_{si}\right]$$

In the above, the 4th equation in both prediction and correction steps is solved by Newton method. Moreover, pressure at the entry plane and velocity at the exit plane are obtained

by extrapolation. The computer code was validated using analytical solutions related to steady-state solutions of the above equations for which we could obtain analytical solutions.

Numerical Solutions

The critical wall shear stress t_a for 40% and unfilled PDMS are 35000 and 70,000 Pa, respectively [Kalyon and Gevgilili (2003); Kalyon et al. (2003)]. Pressure-volume-temperature, P-V-T, experiments were used to determine the compressibility coefficients for the PDMS and 40% by volume glass-filled PDMS. It was determined that $g = 1.6 \times 10^{-6} m \cdot s^{-2}$ and $g_1 = 1073.4 kg \cdot m^{-3}$ for 40% PDMS and $g = 1.4 \times 10^{-6} m \cdot s^{-2}$ and $g_1 = 958.0 kg \cdot m^{-3}$ for PDMS.

a) Suspension of PDMS incorporated with 40% by volume glass spheres

Using a set of capillary flow experimental data at large shear rates, the parameters of 40% PDMS were determined using the inverse problem solution methodologies [Tang and Kalyon (2004)]: $m = 87600 Pa \cdot s^{0.16}$, $n = 0.16$, $t_y = 58800 Pa$, $\beta = 1 \times 10^{-13} m \cdot s^{-1} \cdot Pa^{2.17}$, and $sb = 2.17$. In the low shear rate range (less than 5 s-1) a second set of parameters were found to be applicable [Tang and Kalyon (2004)]: $m = 50000 Pa \cdot s^{0.5}$, $n = 0.5$, $t_y = 403 Pa$, $\beta_0 = 1.05 \times 10^{-14} m \cdot s^{-1} \cdot Pa^{-2.17}$, $k = 0$, and $sb = 2.17$.

Figure 6 shows a typical solution for the suspension of PDMS with 40% glass for pressure, velocity, slip velocity, shear stress under the conditions of 2R=0.0015m, L/2R=40, V₀=0.01m/s. In the figure, triangles represent slip velocity. The figure also

presents the time history of pressure at the entrance and of velocity at the exit. The simulation results indicate that the solution only has a very short transient state and then the solution becomes steady. It is seen that the flow is actually a plug flow, that is $V = u_s$, where V is the average velocity and u_s is the slip velocity. Over the length of the entire tube wall shear stress increases in the axial z-direction. The wall shear stress is always greater than the critical wall shear stress at which the transition between the stick and slip conditions occurs.

The time-dependent simulations of the flow field for all of the conditions pertaining to the flow curve given in Figure 4 were carried out. Over a broad range of conditions the typical behavior observed in Figure 6, summarized as fast conversion of the flow condition into a steady state, and development of a steady slip velocity at the wall and the wall shear stress values always greater than the critical wall shear stress at which the transition from stick to the slip condition occurs was observed. The predicted mean values of the wall shear stress versus the apparent shear rate values are shown in Figure 7. Over a broad range of conditions, except at the lowest shear rates, the simulation suggests that the flow would occur under steady state conditions as indeed observed in the corresponding experiments (no pressure fluctuations and the extrudate surfaces were smooth, i.e., Figure 4). For the lowest shear rates considered such as around 2 s^{-1} the flow was predicted to be unsteady. This is an important finding and suggests that the onset of flow instabilities is predicted for suspensions of PDMS at wall shear stress values which are less than the critical wall shear stress at which strong wall slip is onset. This is indeed the experimental behavior shown in Figure 4.

In the relatively high shear rate range the wall shear stress is greater than the critical shear stress with no crossing-over the critical shear stress. However, in the low shear rate range the wall shear stress values are in the neighborhood of the critical wall shear stress values and the simulations reveal cross-over from below to above the value of the critical shear stress over the length of the die.

What happens if the Navier's slip coefficient is assumed to be pressure dependent? A second set of simulations for the PDMS with 40% by volume glass were carried out using the following dependence of the Navier's slip coefficient on pressure

$$\boldsymbol{b} = \boldsymbol{b}_0 (p_a / p)^k \qquad\qquad (11)$$

and parameters $m = 47600\,Pa \cdot s^{0.15}$, $n = 0.15$, $\boldsymbol{t}_y = 40000\,Pa$, $\beta_0 = 3.5 \times 10^{-13}\,\mathrm{m \cdot s^{-1} \cdot Pa^{-2.17}}$, $\boldsymbol{k} = 0.3$, and $sb = 2.17$.

The results shown in Figure 8 are obtained for 2R=0.0025m, L/2R=60, V₀=0.0125m/s. In the figures, triangles represent slip velocity. The mean velocity values are represented by the continuous curves. Steady state is again achieved very fast (Fig 8). The slip velocity values are relatively large. Under such steady state conditions the time-dependent and steady values of the wall shear stress at various locations in the cylindrical tube are all greater than the critical wall shear stress at which the transition from the stick to the slip condition occurs. The mean values of the wall shear stress under steady state conditions over the entire set of conditions of the experiments and the corresponding experimental values are shown in Figure 9. The predictions and the experiments agree that over a large range of shear rates (apparent shear rates are larger than 10), there are no fluctuations in pressure and the extrudates are smooth and free of any type of surface irregularities,

suggesting that the flow over the entire range of shear rates occurred free of flow instabilities. Overall, the differences between the predictions of the simulations that use the constant or the pressure-dependent Navier's slip coefficient are not significant. The low shear rate region was not probed in these simulations akin to those conditions used to generate the results given in Figure 7.

.

b) Solutions for unfilled PDMS

The typical results of time-dependent solutions of the Poiseuille flow for PDMS obtained for a constant Navier's slip coefficient are shown in Figure 10. In the figure, at shear rates greater than 5 s^{-1}, the parameters collected from the experiments with the higher shear rates were used: $m = 27000 \, Pa \cdot s^{0.15}$, $n = 0.15$, $t_y = 40000 \, Pa$, $\beta = 0.9 \times 10^{-11} \, m \cdot s^{-1} \cdot Pa^{-2.26}$, $sb = 2.26$. For shear rates lower than 5 s^{-1}, parameters collected from the experiments with the lower shears were used: [Tang and Kalyon (2004)]: $m = 17200 \, Pa \cdot s^{0.39}$, $n = 0.39$, $t_y = 0 \, Pa$, $\beta_0 = 4.15 \times 10^{-15} \, m \cdot s^{-1} \cdot Pa^{-2.26}$, $k = 0$, and $sb = 2.26$. The diameter of the tube, the length over the diameter ratio and the initial mean velocity were 2R=0.0025m, L/2R=60, V_0=0.001m/s, respectively. In the figure, triangles represent slip velocity. The pressure exhibits time-dependence and the values of the mean velocity, wall shear stress and the slip velocity at the wall all exhibit time-dependence, which are not damped. The periodicity observed here is typical and persists indefinitely with no steady state solution reached under shear rates, which are greater than 5 s^{-1}.

It is interesting to note that the wall shear stress distribution collected at a value of 100 s upon the inception of the shear flow from the rest state suggests that the critical wall shear stress at which the transition from the stick condition to wall slip occurs is crossed multiple times. The transition from the stick to the slip condition appears to generate the time dependence of the pressure, and location-dependent values of the mean velocity and the slip velocity. The predicted periodicity shown in Figure 10 suggests that the flow would not become steady and would exhibit fluctuations in the pressure necessary to drive the flow on one hand and distortions in the extrudates caused by the time dependent changes in the flow boundary condition at the wall and the location specific values of the mean flow velocity.

Does the nature of the flow change if the Navier's slip coefficient is taken to be dependent on the pressure? A new set of solutions was obtained with the following parameters for unfilled PDMS and are shown in Figure 11. $m = 27000 Pa \cdot s^{0.15}$, $n = 0.15$, $t_y = 35000 Pa$, $\beta_0 = 0.9 \times 10^{-11} \text{m} \cdot \text{s}^{-1} \cdot \text{Pa}^{-2.26}$, $k = 1$, and $sb = 2.26$. Figure 11 again indicates that the wall shear stress oscillates around the critical stress. It also shows that slip-stick prevails and governs the flow behavior, such as sometimes the slip velocity approaches zero, and sometimes it approaches the cross-section averaged mean velocity, thus oscillating between the no slip to unfilled slip (plug flow) conditions.

The simulations were carried out over a broad range of apparent shear rates, i.e., 2-200 s^{-1}. The time-dependence of the velocities and the pressure prevailed over almost this entire range of apparent shear rates, except in the lowest shear rate range of less than 5 s^{-1}. The

time-averaged values of the predicted wall shear stress values are shown in Figure 12. It should be noted again that all of the wall shear stress values shown in Figure 12 for which flow instabilities were predicted are very close to the critical wall shear stress at which the transition from the stick to the slip condition occurs. Thus, for this entire range of apparent shear rates the critical value of the shear stress is encountered at some location at the surface of the die and initiates the flow instability mechanism to give rise to the observed surface irregularities shown in Figure 2. However, at the lowest shear rate considered, i.e., around apparent shear rate of 2 s^{-1} and less, steady solutions were observed (Figure 12). Under these conditions the wall shear stress values are significantly lower than the critical wall shear stress at which strong wall slip is onset in steady torsional flow.

IV. Concluding remarks

A time-dependent solution of the capillary flow of compressible generalized Newtonian fluids subject to wall slip is presented. The model shows that the critical shear stress, at which apparent slip occurs, plays an important role to determine if the capillary flow is steady or unsteady. The numerical findings agree with the experimental findings for the capillary flow of the two materials of our study, i.e., PDMS and filled PDMS.

Overall, these results appear to confirm our earlier hypothesis (Kalyon et al. (2003) that the stability of the wall boundary condition during flow is very important. The critical

wall shear stress at which strong wall slip occurs acts as a boundary. If the flow conditions generate wall shear stress values which are in the neighborhood of this critical wall shear stress than transitions from the steady to unsteady or from unsteady to steady flow occurs. It is also interesting to note that for the filled PDMS a stable wall slip condition (with wall shear stress values significantly greater than the critical shear stress) prevails over the bulk of the flow curve and the flow in this region is steady. Only when the apparent shear rate is sufficiently reduced so that the corresponding wall shear stress values approach the critical wall shear stress then flow instabilities are onset.

For the unfilled PDMS bulk of the flow curve involves wall shear stress values, which are in the neighborhood of the critical wall shear stress, and the flow over this broad range of shear rates is unsteady. The resulting wall slip condition is not stable with non-periodic excursions between the slip and stick conditions. The decrease of the shear rate to lower than $2\ s^{-1}$ for unfilled PDMS gives rise to wall shear stress values that are significantly lower than the critical shear stress and the resulting stable stick condition generates stable flow.

References

Aral, B., Kalyon, D. M. (1994) Effects of temperature and surface roughness on time-dependent wall slip in steady torsional flow of concentrated suspensions. J. Rheol., 38, 957-972.

Aral, B, Kalyon, D. M. (1995) Rheology and Extrudability of Very Concentrated Suspensions: Effects of Vacuum Imposition. Plast. and Rubber Comp. Proc. and Applications, 24, 201-210.

Benbow, J. J. and P. Lamb, "New aspects of melt fracture," SPE Transactions **3**, 7-17 (1963).

Denn M. M. (2001) Extrusion instabilities and wall slip, Annu. Rev. Fluid Mech., 33, 265-287

Donlder C. F. J. den, Koopmans, R. J., Molenaar, J (1998) Quantitative modeling of HDPE spurt experiments using wall slip and generalized Newtonian flow, J. Non-Newtonain Fluid Mech., 79, 503-514

Gevgilili, H. and Kalyon D. M. (2001) Step strain flow: wall slip effects and other error sources. J. Rheol. **45**, 1-9.

Georgiou, G. C. (2003) The time-dependent, compressible Posiseuille and extrusion-swell flows of a Carreau fluid with slip at wall, J. Non-Newtonian Fluid Mech., 109, 93-114.

Hatzikiriakos, S. G. and Dealy, J. M. (1992a) Role of slip and fracture in the oscillating flow of HDPE in a capillary. J. Rheol., 36, 845-884

Hatzikiriakos, S. G. and Dealy, J. M. (1992b) Wall slip of molten high density polyethylenes.II. Capillary rheometer studies, J. Rheol., 36, 4, 703-741.

Kalyon, DS. M., Yaras, P., Aral, B., Yilmazer, U. (1993) Rheological behavior of a concentrated suspension: A solid rocket fuel simulant, J. Rheo., 37, 35-53

Kalyon, D., H. Gokturk, P. Yaras, Aral B. (1995) Motion Analysis of Development of Wall Slip During Die Flow of Concentrated Suspensions. Society of Plastics Engineers ANTEC Technical Papers, 41, 1130-1134.

Kalyon, D. M., Gevgilili H. (2003) Wall slip and extrudate distortion of three polymer melts. J. Rheol., 47, 3, 683-699.

Kalyon, D. M, Birinci, E. and Gevgilili, H.(2003) Development of extrudate distortions as affected by wall slip behavior of polymers and filled polymers.

Proceedings of Annual Meeting of American Institute of Chemical Engineers Annual Meeting.

Lim, F. J., Schowalter, W. R. (1989) Wall slip of narrow molecular weight distribution polybutadienes, 33, 1360-1382

Ovaici, H., Mackley, M. R., McKinley, G. H., Crook, S. J. (1998) The experimental observation and modeling of an "Ovaici" necklace and stick-spurt instability arising during the cold extrusion of chocolate, J. Rheol., 42, 125-157

Petrie, C. J. S. and M. M. Denn, "Instabilities in polymer processing," AIChE J. **22**, 209-236 (1976).

Tang, H. S., Kalyon, D. M. (2004) Estimation of the parameters of Herschel-Bulkley fluid under wall slip using a combination of capillary and squeeze flow viscometers, Rheol. Acta 43, 80-88.

Yilmazer, U., Kalyon, D. M. 1989 Slip effects in capillary and parallel disk torsional flows of highly filled suspensions. J. Rheol. 33, 1197-1212

Zhang, W., Silvi, N., Vlachopoulos J. (1995) Modeling and experiments of squeezing flow of polymer melts. Intern. Polymer processing, X, 155-164
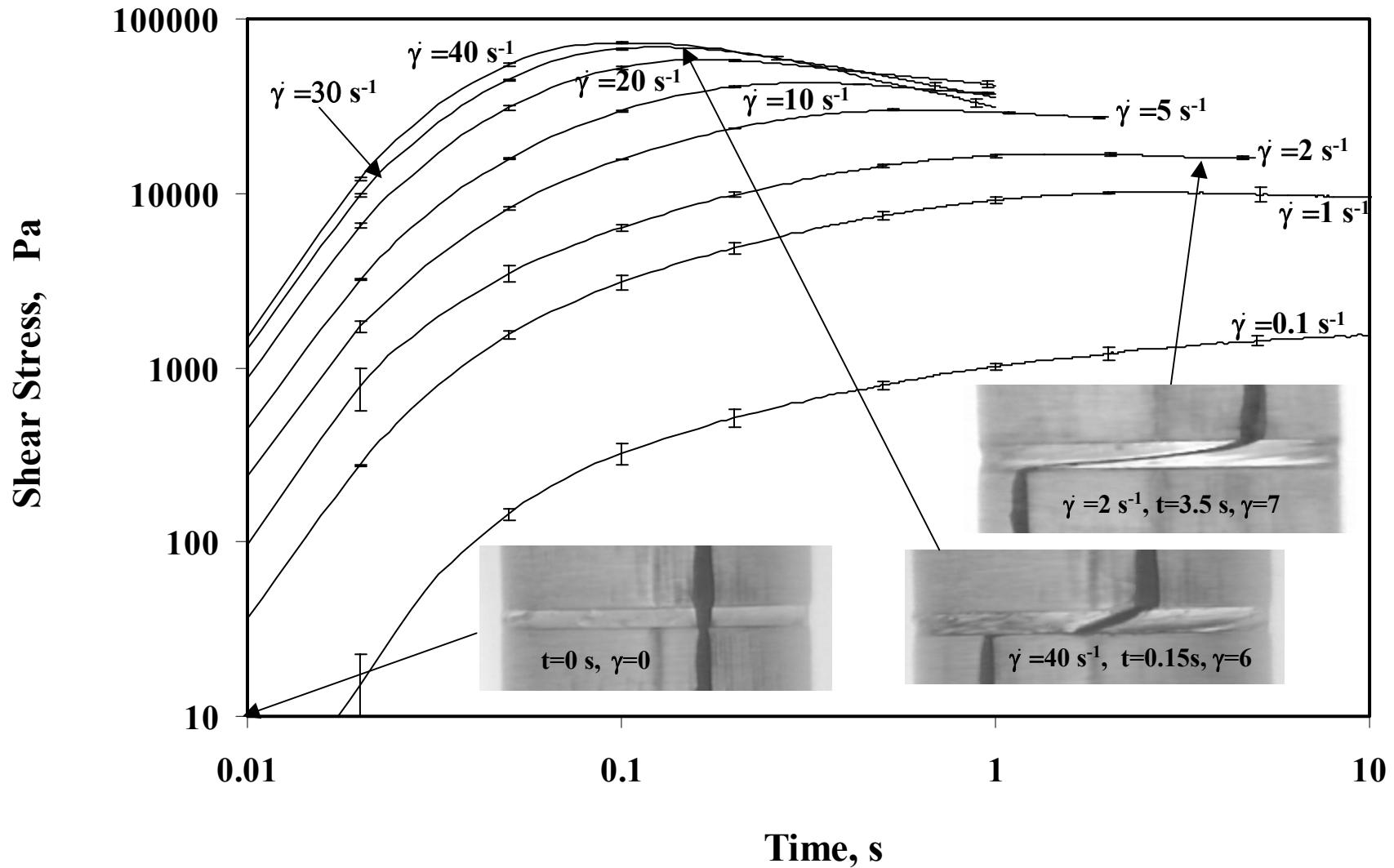
List of figures:

Figure 1 Steady torsional flow of poly(dimethyl siloxane) at various apparent shear rates and results of straight-line marker technique applied at the free surface of PDMS for detection of conditions under which wall slip is initiated.
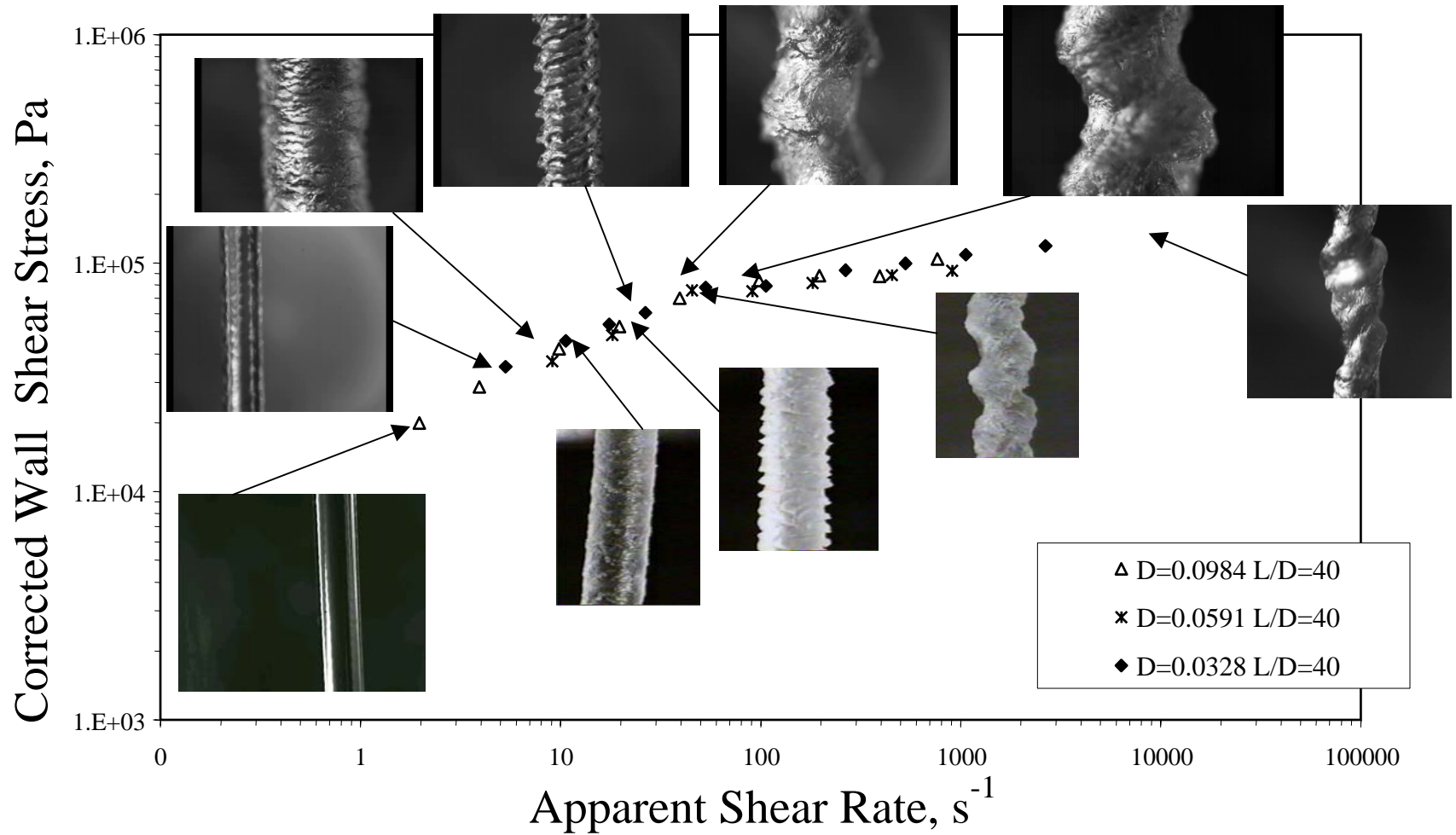
Figure 2. Flow curves and extrudates of poly(dimethyl siloxane) collected with capillaries with different diameters and development of extrudate surface irregularities
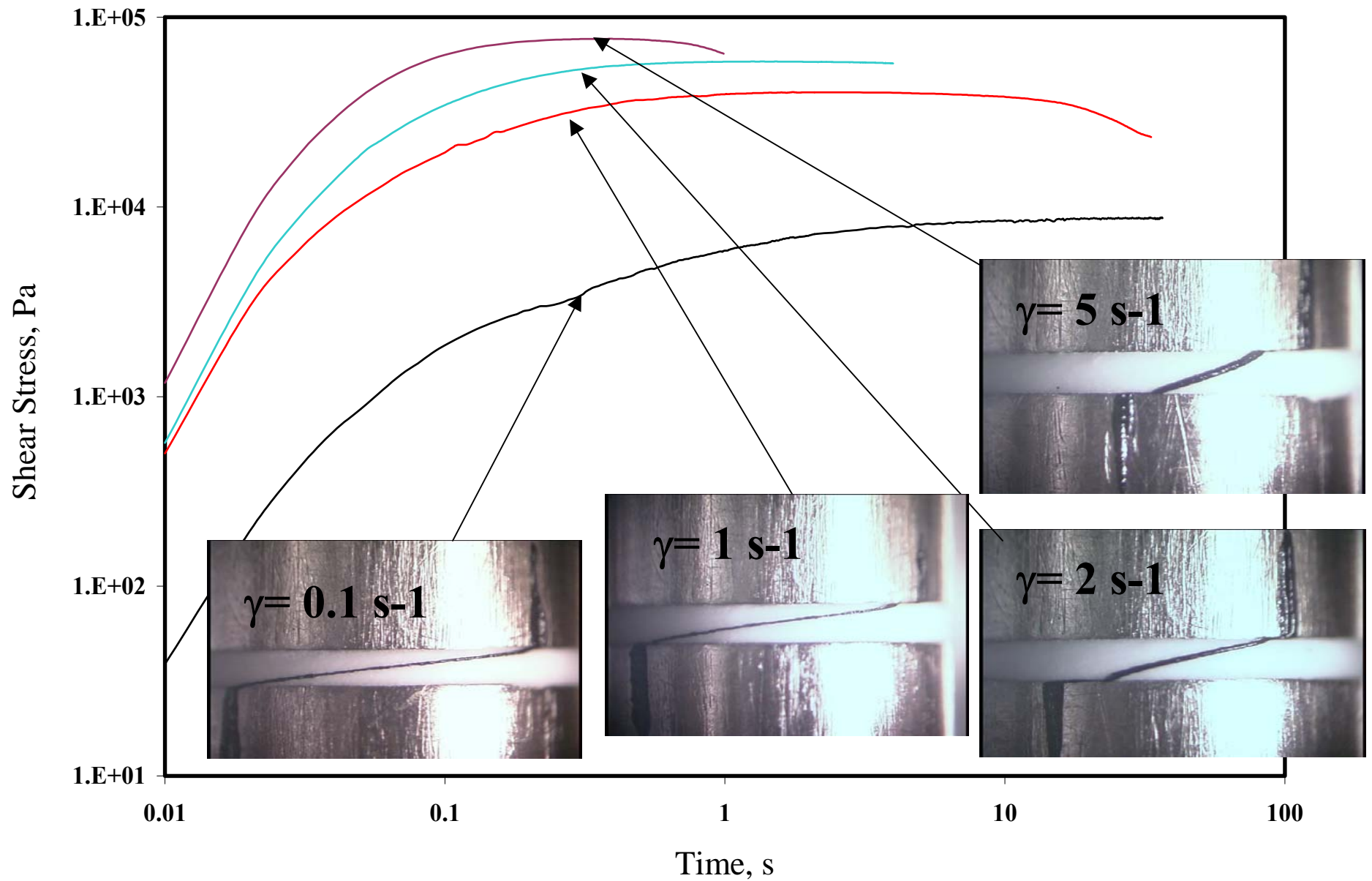
Figure 3 Steady torsional flow of poly (dimethyl siloxane) with 40% glass spheres at various apparent shear rates and results of straight-line marker technique applied at the free surface of 40% filled PDMS
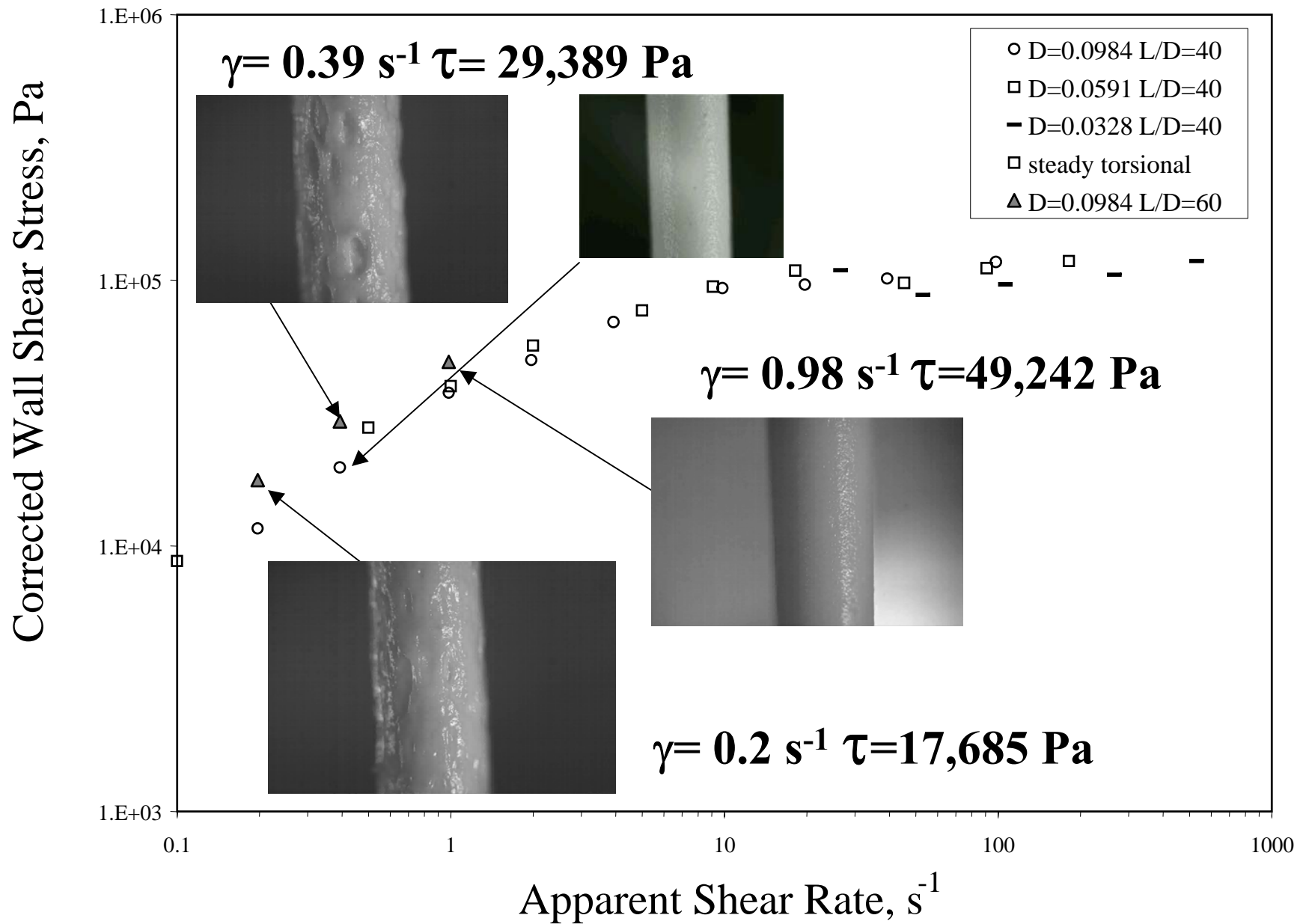
Figure 4 Flow curves and extrudates of suspension of poly(dimethyl siloxane) PDMS incorporated with 40% by volume of glass spheres collected with capillaries with different diameters.
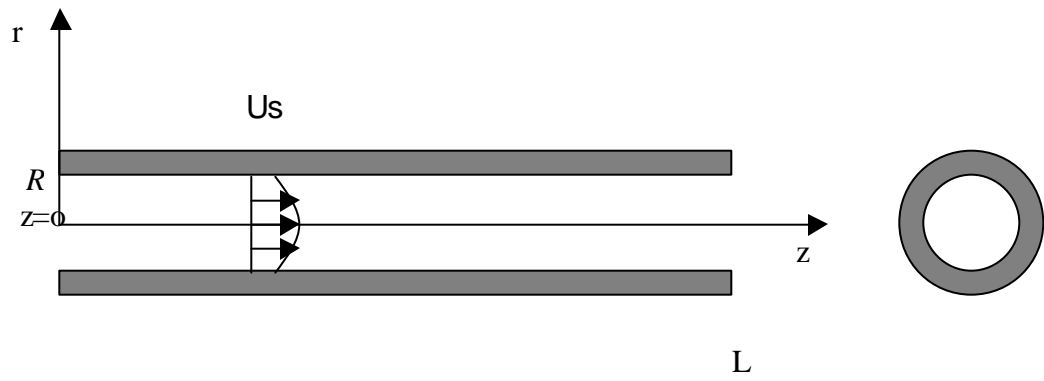
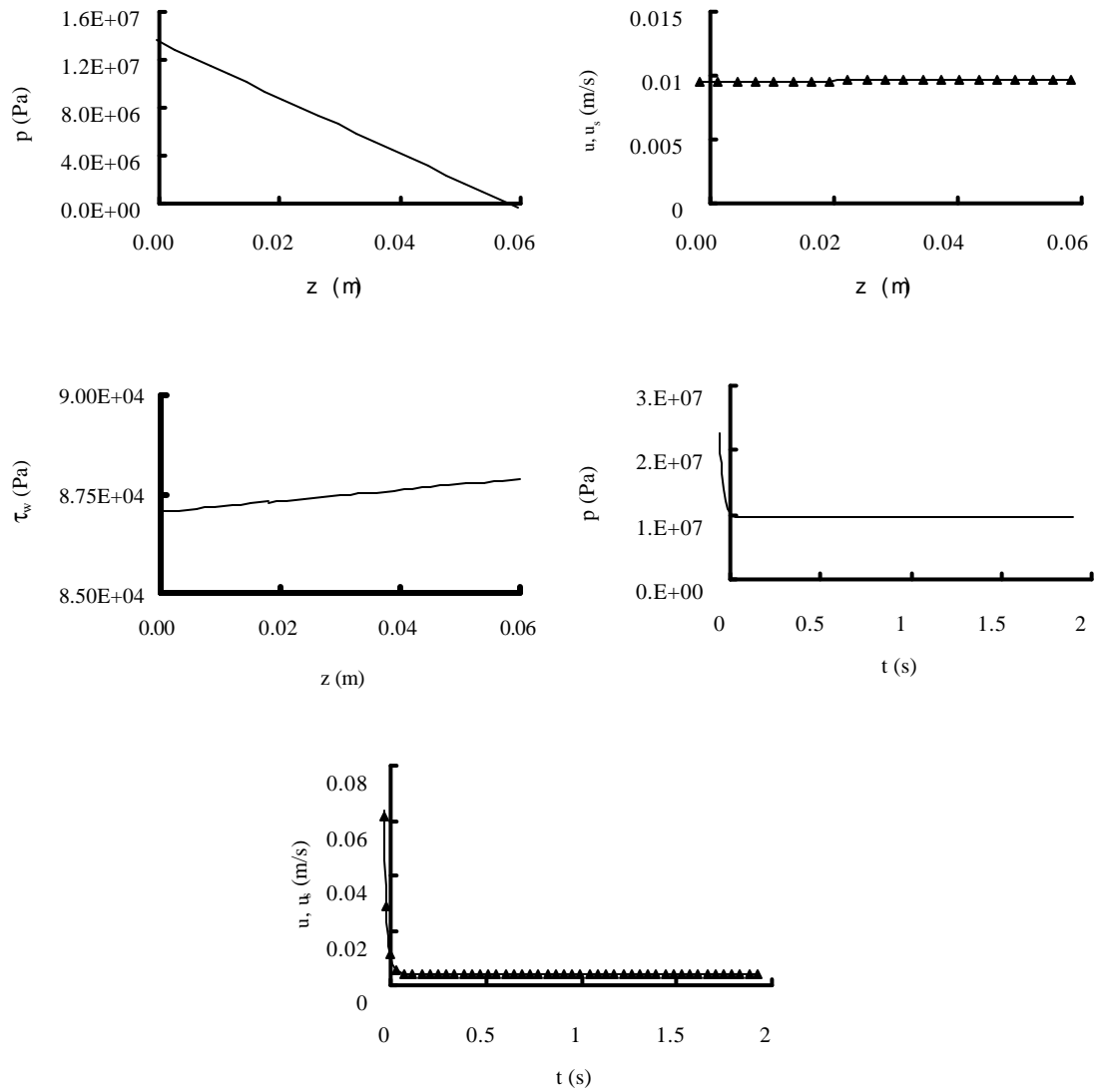Figure 5 Flow through a circular tube (Poiseuille flow) subject to wall slip

Figure 6 Solution for flow of PDMS suspension with 40% by volume of glass spheres using a constant Navier's slip coefficient. $2R=0.0015m$, $L/2R=40$, $V_0=0.01m/s$. In the figure, triangles represent slip velocity.

Figure 7 Predictions for 40% PDMS flows for Navier's slip coefficient, β, equal to a constant and not dependent on pressure. Filled symbols – prediction, hollow symbols—experiment. Squares – $2R=0.0015m$, $L/2R=40$, diamonds – $2R=0.0025m$, $L/2R=60$.

Figure 8 Solutions for 40% PDMS flow with a pressure-dependent slip coefficient. $2R=0.0025m$, $L/2R=60$, $V_0=0.0125m/s$. In the figure, triangles represent slip velocity.

Figure 9.   Predictions for PDMS suspension with 40% glass, using a pressure-dependent slip coefficient. Squares – $2R=0.0015m$, $L/2R=40$, diamonds – $2R=0.0025m$, $L/2R=60$.

Figure 10 Solution of a unfilled PDMS flow with a constant slip coefficient. $2R=0.0025m$, $L/2R=60$, $V_0=0.001m/s$. In the figure, triangles represent slip velocity.

Figure 11 Solution of a unfilled PDMS flow with a pressure dependent slip coefficient. $2R=0.0025m$, $L/2R=60$, $V_0=0.06m/s$. In the figure, triangles represent slip velocity.

Figure 12   Predicted shear stress at the wall versus the apparent shear rate for unfilled PDMS Squares – $2R=0.0015m$, $L/2R=40$, diamonds – $2R=0.0025m$, $L/2R=60$.

Fig. 1 Steady torsional flow of poly(dimethyl siloxane) at various apparent shear rates and results of straight-line marker technique applied at the free surface of PDMS for detection of conditions under which wall slip is initiated.

Fig. 2. Flow curves and extrudates of poly(dimethyl siloxane) collected with capillaries with different diameters and development of extrudate surface irregularities

Fig. 3 Steady torsional flow of poly (dimethyl siloxane) with 40% glass spheres at various apparent shear rates and results of straight-line marker technique applied at the free surface of 40% filled PDMS

Fig. 4 Flow curves and extrudates of suspension of poly(dimethyl siloxane) PDMS incorporated with 40% by volume of glass spheres collected with capillaries with different diameters.

Fig. 5 Flow through a circular tube (Poiseuille flow) subject to wall slip

Fig. 6 Solution for flow of PDMS suspension with 40% by volume of glass spheres using a constant Navier's slip coefficient. 2R=0.0015m, L/2R=40, V_0=0.01m/s. In the figure, triangles represent slip velocity.
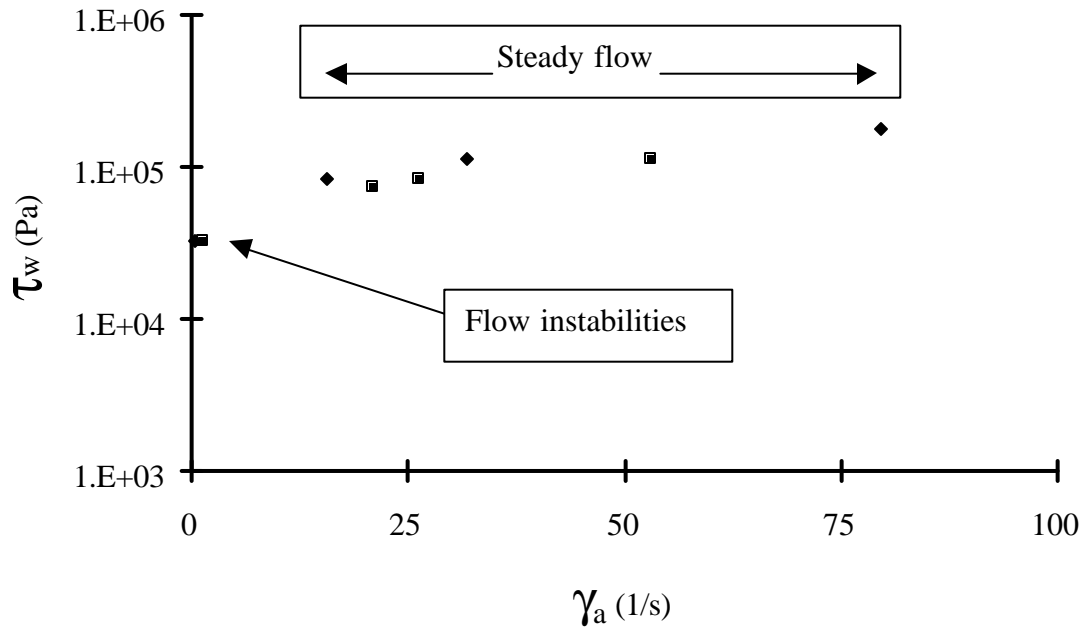
Fig. 7 Predictions for 40% PDMS flows for Navier's slip coefficient, β, equal to a constant and not dependent on pressure. Filled symbols – prediction, hollow symbols— experiment. Squares – 2R=0.0015m, L/2R=40, diamonds – 2R=0.0025m, L/2R=60.
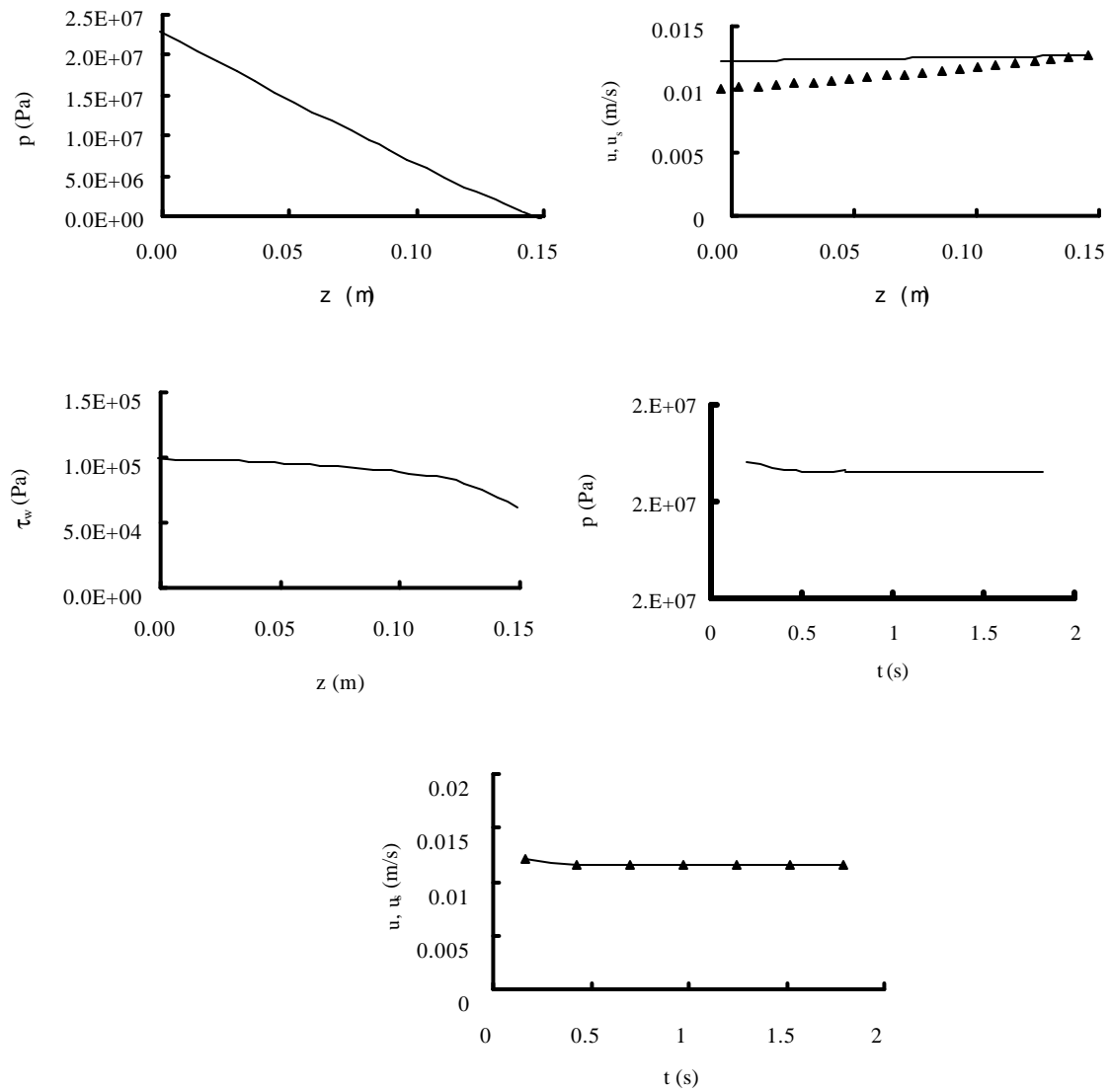
Fig. 8 Solutions for 40% PDMS flow with a pressure-dependent slip coefficient. 2R=0.0025m, L/2R=60, V$_0$=0.0125m/s. In the figure, triangles represent slip velocity.
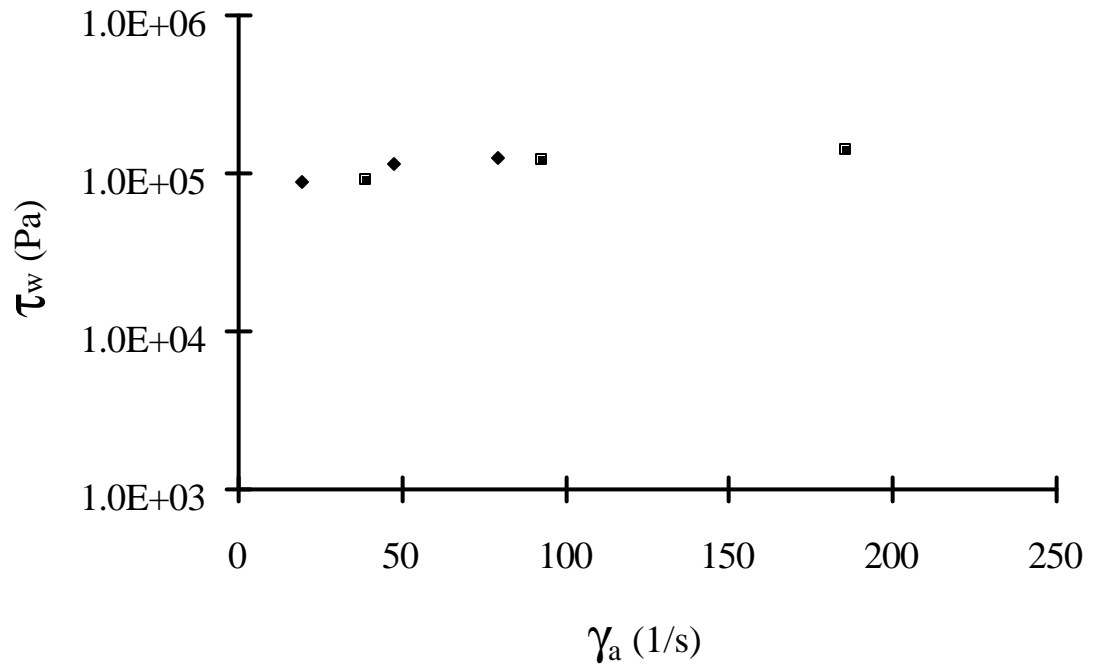
Fig. 9.   Predictions for PDMS suspension with 40% glass, using a pressure-dependent slip coefficient. Squares – 2R=0.0015m, L/2R=40, diamonds – 2R=0.0025m, L/2R=60.
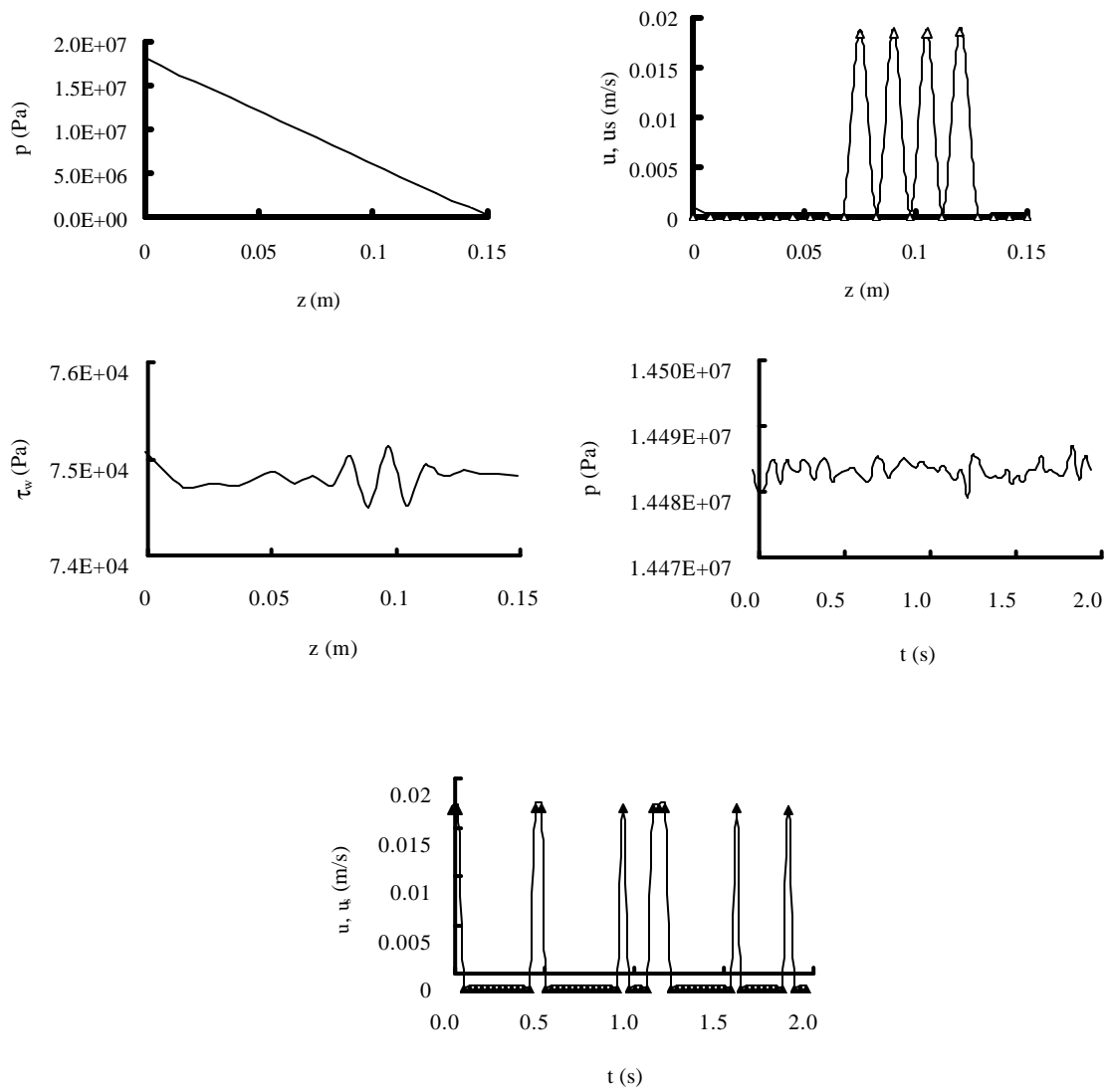
Fig. 10 Solution of a pure PDMS flow with a constant slip coefficient. 2R=0.0025m, L/2R=60, V_0=0.001m/s. In the figure, triangles represent slip velocity.
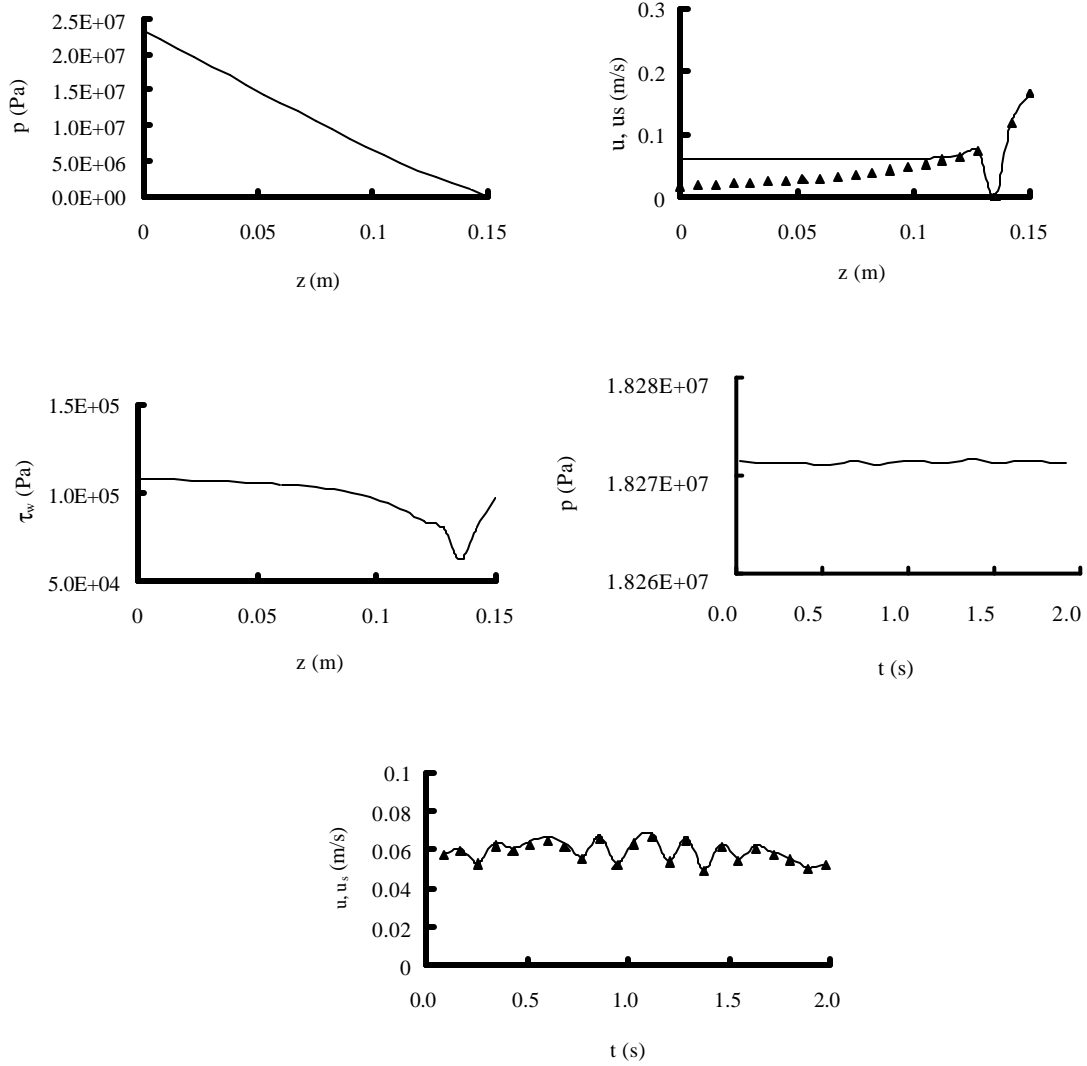
Fig. 11 Solution of a pure PDMS flow with a pressure dependent slip coefficient. 2R=0.0025m, L/2R=60, V₀=0.06m/s. In the figure, triangles represent slip velocity.
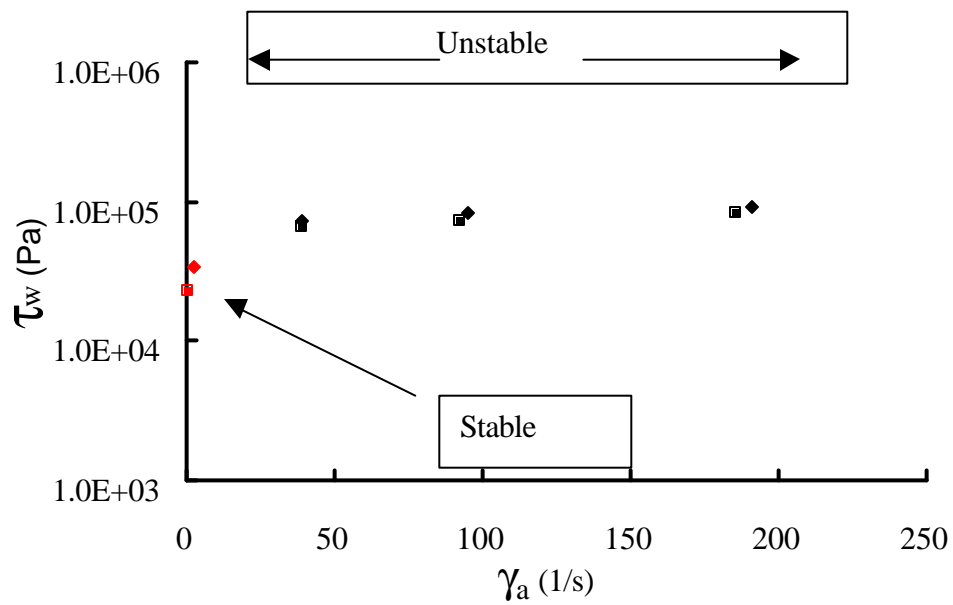
Fig. 12   Predicted shear stress at the wall versus the apparent shear rate for pure PDMS
Squares – 2R=0.0015m, L/2R=40, diamonds – 2R=0.0025m, L/2R=60.